

# Spectroscopy of “Big Trio” Objects Using the “Scorpio” Spectrograph of the 6-m Telescope of the Special Astrophysical Observatory <sup>\*</sup>

Yu. N. Parijskij<sup>1</sup>, A. I. Kopylov<sup>1</sup>, A. V. Temirova<sup>2</sup>, N. S. Soboleva<sup>2</sup>, O. P. Zhelenkova<sup>1</sup>, O. V. Verkhodanov<sup>1</sup>, W. M. Goss<sup>3</sup>, T. A. Fatkhullin<sup>1</sup>

<sup>1</sup> Special Astrophysical Observatory, Russian Academy of Sciences, Nizhnij Arkhyz, Karachaj-Cherkessian Republic, 357147 Russia

<sup>2</sup> St. Petersburg Branch of the Special Astrophysical Observatory, Russian Academy of Sciences, Pulkovskoe sh. 65, St. Petersburg, 196140 Russia

<sup>3</sup> National Radio Astronomy Observatory, P. O. Box O, 1003 Lopezville Road, Socorro, NM 87801-0387, USA

*Received February 1, 2010; accepted February 5, 2010.*

**Abstract.** We present the results of spectroscopy of 71 objects with steep and ultra-steep spectra ( $\alpha < -0.9$ ,  $S \propto \nu^\alpha$ ) from the “Big Trio” (RATAN-600–VLA–BTA) project, performed with the “Scorpio” spectrograph on the 6-m telescope of the Special Astrophysical Observatory (Russian Academy of Sciences). Redshifts were determined for these objects. We also present several other parameters of the sources, such as their Rmagnitudes, maximum radio sizes in seconds of arc, flux densities at 500, 1425, and 3940 MHz, radio luminosities at 500 and 3940 MHz, and morphology. Of the total number of radio galaxies studied, four have redshifts  $1 < z < 2$ , three have  $2 < z < 3$ , one has  $3 < z < 4$ , and one has  $z = 4.51$ . Thirteen sources have redshifts  $0.7 < z < 1$  and 15 have  $0.2 < z < 0.7$ . Of all the quasars studied, five have redshifts  $0.7 < z < 1$ , seven have  $1 < z < 2$ , four have  $2 < z < 3$ , and one has  $z = 3.57$ . We did not detect any spectral lines for 17 objects.

**DOI:** 10.1134/S1063772910080019

## 1. INTRODUCTION

The “Big Trio”<sup>5</sup> project, which was initiated in 1991-1992 [1] and is based on three large instruments — the RATAN-600, the VLA, and the 6-m optical telescope of the Special Astrophysical Observatory (SAO) – is aimed at searching for and studying very distant radio galaxies. (For a detailed description of the project, see the book by Verkhodanov and Pariiskii [2].) The project was carried out in several stages. The first stage – a search survey with the RATAN-600 radio telescope in 1980-1981 (the “Kholod” experiment [3, 4]) – resulted in the RC catalog [5, 6] at 3940 MHz, which also made use of the Texas catalog at 365 MHz<sup>1</sup> to obtain a sample the Texas catalog at 365 MHz<sup>1</sup> to obtain a sample of objects with steep and ultra-steep spectra. (The steepness of the radio spectrum was already known to be useful for selecting very distant objects [7, 8].)

The next stage was to study the structure of the sample objects with the VLA at 1425 and 4885 MHz. This made it possible to identify FRII sources – the most energetic radio galaxies, associated with gE giant elliptical galaxies – and to improve their coordinates.

The third stage was optical identification of the radio sources: for bright sources, from the Palomar prints and, for fainter ones, from R-band observations with the 6-m telescope of the SAO [9-11]. We studied the optical structures of some objects with a resolution of  $<1''$  using the NOT (Nordic Optical Telescope, Canary Islands) [12].

To derive the spectral energy distributions of the host galaxies based on evolutionary models, the fourth stage included BVRI-photometry with the 6-meter SAO telescope [13, 14]. These data were used to obtain photometric redshifts and estimate the ages of the host galaxies.

In the last stage, we determined spectroscopic redshifts, first with the multi-pupil spectrograph [15] and then with the “Scorpio” spectrograph (mounted on the 6-m telescope of the SAO) [16].

The results for all previous stages were published earlier [9–27]. In this paper, we present the results of the last stage: spectroscopic redshifts derived from observations with the “Scorpio” spectrograph (on the 6-m telescope of the SAO).

## 2. OBSERVATIONAL RESULTS

The data obtained from our observations with the “Scorpio” spectrograph mounted on the 6-m SAO telescope are collected in four tables. In total, we studied 71 objects with steep and ultra-steep spectra from the RC catalog. These include 17 quasars, with the other objects being radio galaxies. Tables 1 and 2 present the results for radio galaxies with detected emission lines, subdivided according to their redshifts. Table 1 contains 22 radio galaxies with redshifts  $z > 0.7$ , and Table 2 – 15 radio galaxies with redshifts between 0.2 and 0.7.

The columns of Tables 1 and 2 contain for each object: 1 — a running number; 2 — the name in the RC catalog; 3, 4 — the right ascension and declination of the object for equinox 2000; 5 — the R-band magnitude; 6 — the spectroscopic redshift ( $z_{sp}$ ); 7 — the largest angular size in arcseconds, LAS; 8, 9, 10 — the flux densities  $S$ , in mJy, at 3940, 1400, and 500 MHz (the last obtained from interpolating the spectrum); 11, 12 — the spectral indices  $\alpha$  ( $S \propto \nu^\alpha$ ) at 3940 and 500 MHz; 13, 14 — the luminosities  $L$ ,  $W \text{ Hz}^{-1}$ , at 3940 and 500 MHz; 15 — the radio source morphology, with ‘P’ denoting a point-like object, ‘D’ a double

---

<sup>1</sup> Kindly provided by Prof. J. Douglas prior to its publication.

Table 1. Radio galaxies with  $z > 0.7$ .

| No. | RCJ name  | RA  | Dec         | $m_R$ | $z_{sp}$ | LAS   | $S'_{3940}$<br>mJy | $S'_{1400}$<br>mJy | $S'_{500}$<br>mJy |
|-----|-----------|---|-------------|-------|----------|-------|--------------------|--------------------|-------------------|
| 1   | 2         | 3   | 4           | 5     | 6        | 7     | 8                  | 9                  | 10                |
| 1   | 0015+0501 | 00 <sup>h</sup> 15 <sup>m</sup> 22.8 <sup>s</sup> | 05°01'22.4" | 23.2  | 0.813    | 20.1" | 34                 | 110                | 295               |
| 2   | 0034+0513 | 00 34 06.24                                       | 05 14 57.6  | 23.3  | 0.962    | 12.1  | 93                 | 252                | 605               |
| 3   | 0105+0501 | 01 05 34.46                                       | 05 01 09.8  | 22.8  | 3.138    | 7.6   | 27                 | 92                 | 285               |
| 4   | 0213+0516 | 02 13 36.25                                       | 05 18 19.2  | 22.1  | 0.935    | 36.8  | 143                | 425                | 963               |
| 5   | 0225+0506 | 02 25 09.75                                       | 05 08 37.4  | 22.1  | 0.770    | 0.2   | 82                 | 239                | 586               |
| 6   | 0311+0507 | 03 11 47.99                                       | 05 08 04.1  | 22.9  | 4.514    | 2.8   | 135                | 537                | 1711              |
| 7   | 0444+0501 | 04 44 17.93                                       | 05 01 25.7  | 23.0  | 1.820    | 11.1  | 70                 | 206                | 553               |
| 8   | 0506+0508 | 05 06 25.00                                       | 05 08 19.3  | 21.6  | 0.817    | 0.8   | 91                 | 221                | 427               |
| 9   | 0744+0500 | 07 44 52.63                                       | 05 00 09.4  | >24.5 | 2.48     | 10.8  | 28                 | 99                 | 341               |
| 10  | 0837+0446 | 08 37 29.37                                       | 04 44 21.8  | 22.2  | 1.769    | 3.9   | 62                 | 164                | 384               |
| 11  | 0909+0445 | 09 09 51.09                                       | 04 44 22.9  | 20.6  | 0.753    | 0.1   | 70                 | 192                | 472               |
| 12  | 1322+0449 | 13 22 03.48                                       | 04 48 50.5  | 20.4  | 0.799    | 1.7   | 46                 | 115                | 269               |
| 13  | 1339+0445 | 13 39 37.85                                       | 04 55 04.3  | 22.3  | 0.740    | 34.0  | 40                 | 126                | 290               |
| 14  | 1357+0453 | 13 57 37.39                                       | 04 53 16.1  | 21.3  | 0.864    | 12.4  | 91                 | 250                | 584               |
| 15  | 1503+0456 | 15 03 59.70                                       | 04 56 50.4  | 22.8  | 0.788    | 4.5   | 64                 | 199                | 545               |
| 16  | 1510+0438 | 15 10 12.67                                       | 04 39 31.5  | 22.1  | 0.870    | 3.4   | 71                 | 154                | 318               |
| 17  | 1626+0448 | 16 26 50.29                                       | 04 48 51.3  | 22.9  | 2.656    | 2.4   | 57                 | 200                | 564               |
| 18  | 1638+0450 | 16 38 32.21                                       | 04 49 56.3  | 22.3  | 1.272    | 1.9   | 177                | 436                | 1680              |
| 19  | 2029+0456 | 20 29 43.40                                       | 04 56 11.3  | 21.7  | 0.789    | 28.9  | 73                 | 153                | 364               |
| 20  | 2224+0513 | 22 24 17.89                                       | 05 13 47.3  | 21.3  | 0.974    | 36.1  | 120                | 328                | 790               |
| 21  | 2247+0507 | 22 47 15.18                                       | 05 08 09.0  | 22.1  | 1.055    | 5.6   | 120                | 347                | 885               |
| 22  | 2348+0507 | 23 48 32.01                                       | 05 07 33.8  | 22.8  | 2.014    | 4.7   | 145                | 399                | 1151              |

| No. | $\alpha_{3940}$ | $\alpha_{500}$ | $L_{3940}$<br>WHz <sup>-1</sup> | $L_{500}$<br>WHz <sup>-1</sup> | Morphology  | Note            |
|-----|-----------------|----------------|---------------------------------|--------------------------------|-------------|-----------------|
| 1   | 11              | 12             | 13                              | 14                             | 15          | 16              |
| 1   | -1.221          | -0.84          | $8.77 \times 10^{25}$           | $5.96 \times 10^{26}$          | T,BC,FRII   | abs             |
| 2   | -0.817          | -1.031         | $2.63 \times 10^{26}$           | $1.98 \times 10^{27}$          | D,FRII      | abs             |
| 3   | -1.154          | -1.142         | $1.66 \times 10^{27}$           | $1.57 \times 10^{28}$          | CL          | n(Ly $\alpha$ ) |
| 4   | -0.925          | -0.925         | $4.12 \times 10^{26}$           | $3.21 \times 10^{27}$          | T,C,FRII    | abs             |
| 5   | -1.091          | 0.789          | $1.70 \times 10^{26}$           | $1.23 \times 10^{27}$          | P           | BLRG; B + abs   |
| 6   | -1.366          | -1.095         | $2.38 \times 10^{28}$           | $3.19 \times 10^{29}$          | T,BC,FRII   | n(Ly $\alpha$ ) |
| 7   | -1.098          | -0.911         | $1.02 \times 10^{27}$           | $8.13 \times 10^{27}$          | D,FRII      | n               |
| 8   | -0.961          | -0.531         | $1.99 \times 10^{26}$           | $7.24 \times 10^{26}$          | D,FRII      | abs             |
| 9   | -1.275          | -1.095         | $7.33 \times 10^{26}$           | $1.02 \times 10^{28}$          | D,FRII      | n(Ly $\alpha$ ) |
| 10  | -0.945          | -0.83          | $7.46 \times 10^{26}$           | $4.39 \times 10^{27}$          | D, FRII     | BLRG            |
| 11  | -0.927          | -0.927         | $1.26 \times 10^{26}$           | $8.52 \times 10^{26}$          | P           | n               |
| 12  | -0.977          | 0.735          | $9.71 \times 10^{25}$           | $4.93 \times 10^{26}$          | T,BC,FRII/I | abs             |
| 13  | -1.1            | -0.806         | $7.74 \times 10^{25}$           | $4.71 \times 10^{26}$          | D,FRII      | n               |
| 14  | -0.899          | -0.899         | $2.18 \times 10^{26}$           | $1.39 \times 10^{27}$          | D,FRII      | n               |
| 15  | -1.208          | -0.860         | $1.51 \times 10^{26}$           | $1.04 \times 10^{27}$          | CJ          | BLRG;B+abs      |
| 16  | -0.728          | -0.728         | $1.54 \times 10^{26}$           | $6.91 \times 10^{26}$          | D,FRII      | n+abs           |
| 17  | -1.176          | -1.047         | $2.22 \times 10^{27}$           | $1.87 \times 10^{28}$          | D,FRII      | n(Ly $\alpha$ ) |
| 18  | -0.875          | -0.875         | $9.53 \times 10^{26}$           | $5.82 \times 10^{27}$          | T,BC,FRII   | n               |
| 19  | -0.78           | -0.78          | $1.34 \times 10^{26}$           | $6.66 \times 10^{26}$          | T,BC,FRII   | n               |
| 20  | -1.032          | -0.796         | $3.65 \times 10^{26}$           | $2.66 \times 10^{27}$          | D,FRII      | n               |
| 21  | -0.966          | -0.966         | $4.63 \times 10^{26}$           | $3.40 \times 10^{27}$          | D,C?,FRII   | BLRG            |

Table 2. Radio galaxies with  $z < 0.7$ .

| No. | RCJ name   | RA   | Dec         | $m_R$ | $z_{sp}$ | LAS   | $S_{3940}$<br>mJy | $S_{1400}$<br>mJy | $S_{500}$<br>mJy |
|-----|------------|--|-------------|-------|----------|-------|-------------------|-------------------|------------------|
| 1   | 2          | 3  | 4           | 5     | 6        | 7     | 8                 | 9                 | 10               |
| 1   | 0110+0500  | 01 <sup>h</sup> 10 <sup>m</sup> 13.91 <sup>s</sup> | 04°59'57.6" | 21.3  | 0.633    | 74.4" | 94                | 247               | 566              |
| 2   | 0135+0450  | 01 35 37.20  | 04 48 33.8  | 18.4  | 0.372    | 7.8   | 101               | 255               | 665              |
| 3   | 0209+0501A | 02 09 12.56  | 05 00 52.2  | 18.5  | 0.285    | 0.4   | 33.4              | 86                | 242              |
| 4   | 0457+0452  | 04 57 53.86  | 04 53 53.5  | 19.4  | 0.482    | 67    | 72                | 199               | 461              |
| 5   | 0820+0454  | 08 20 56.7   | 04 54 16.8  | 19.3  | 0.539    | 2.0   | 165               | 465               | 1206             |
| 6   | 0845+0444  | 08 45 31.20  | 04 42 54.9  | 21.4  | 0.650    | 7.6   | 156               | 504               | 1164             |
| 7   | 0908+0451  | 09 08 21.01  | 04 50 58.3  | 19.6  | 0.525    | 34.5  | 111               | 263               | 700              |
| 8   | 1011+0502  | 10 12 04.58  | 05 06 14.2  | 22.4  | 0.456    | 1.3   | 68                | 210               | 545              |
| 9   | 1124+0456  | 11 24 37.43  | 04 56 18.7  | 17.3  | 0.284    | 12.0  | 440               | 991               | 2716             |
| 10  | 1142+0455  | 11 42 20.10  | 04 54 56.0  | 21.0  | 0.605    | 18.7  | 107               | 292               | 652              |
| 11  | 1155+0444  | 11 55 19.24  | 04 43 31.3  | 18.6  | 0.289    | 13.0  | 71                | 159               | 353              |
| 12  | 1235+0435  | 12 35 49.52  | 04 32 56.9  | 21.5  | 0.657    | 9.1   | 61                | 153               | 300              |
| 13  | 1446+0507  | 14 46 17.97  | 05 07 41.1  | 19.3  | 0.273    | 68.0  | 163               | 364               | 746              |
| 14  | 1646+0501  | 16 46 53.31  | 05 01 10.0  | 21.2  | 0.690    | 15.7  | 55                | 106               | 313              |
| 15  | 1722+0442  | 17 22 14.06  | 04 43 17.0  | 20.7  | 0.604    | 21.9  | 266               | 768               | 2049             |

| No. | $\alpha_{3940}$ | $\alpha_{500}$ | $L_{3940}$<br>WHZ <sup>-1</sup> | $L_{500}$<br>WHZ <sup>-1</sup> | Morphology | Note       |
|-----|-----------------|----------------|---------------------------------|--------------------------------|------------|------------|
| 1   | 11              | 12             | 13                              | 14                             | 15         | 16         |
| 1   | -0.994          | -0.744         | $1.20 \times 10^{26}$           | $6.46 \times 10^{26}$          | D,FRII     | n+abs      |
| 2   | -0.955          | -0.88          | $4.02 \times 10^{25}$           | $2.53 \times 10^{26}$          | TB,C,FRII  | n+abs      |
| 3   | -0.96           | -0.96          | $8.20 \times 10^{24}$           | $4.53 \times 10^{25}$          | P          | abs        |
| 4   | -1.059          | -0.731         | $5.27 \times 10^{25}$           | $2.97 \times 10^{26}$          | D,FRII/I   | n+abs      |
| 5   | -0.993          | -0.993         | $1.50 \times 10^{26}$           | $1.09 \times 10^{27}$          | D,FRII     | n          |
| 6   | -1.19           | -0.753         | $2.34 \times 10^{26}$           | $1.34 \times 10^{27}$          | T,C,FRII   | n+abs      |
| 7   | -0.944          | -0.845         | $9.28 \times 10^{25}$           | $5.64 \times 10^{26}$          | T,C,FRII   | BLRG;B+abs |
| 8   | -1.01           | -1.01          | $4.34 \times 10^{25}$           | $3.47 \times 10^{26}$          | CL         | n          |
| 9   | -0.914          | -0.849         | $1.00 \times 10^{26}$           | $6.18 \times 10^{26}$          | D,FRII     | n+abs      |
| 10  | -0.874          | -0.874         | $1.18 \times 10^{26}$           | $7.16 \times 10^{26}$          | T,C,FRII   | n+abs      |
| 11  | -0.778          | -0.778         | $1.61 \times 10^{25}$           | $8.05 \times 10^{25}$          | D,FRII     | n+abs      |
| 12  | -0.822          | -0.720         | $7.80 \times 10^{25}$           | $3.64 \times 10^{26}$          | D,FRII     | abs        |
| 13  | -0.736          | -0.736         | $3.27 \times 10^{25}$           | $1.50 \times 10^{26}$          | T,WC,FRII  | n+ab       |
| 14  | -0.84           | -0.84          | $7.85 \times 10^{25}$           | $4.47 \times 10^{26}$          | D,FRII     | abs        |
| 15  | -1.061          | -0.918         | $3.18 \times 10^{26}$           | $2.29 \times 10^{27}$          | D,FRII     | n+abs      |

Table 3. Quasars.

| No. | RCJ name  | RA   | Dec         | $m_R$ | $z_{sp}$ | LAS  | $S_{3940}$<br>mJy | $S_{1400}$<br>mJy | $S_{500}$<br>mJy |
|-----|-----------|--|-------------|-------|----------|------|-------------------|-------------------|------------------|
| 1   | 2         | 3  | 4           | 5     | 6        | 7    | 8                 | 9                 | 10               |
| 1   | 0038+0449 | 00 <sup>h</sup> 38 <sup>m</sup> 34.65 <sup>s</sup> | 04°50'50.5" | 2.446 | 3.3'     | 21.2 | 94                | 239               | 640              |
| 2   | 0042+0504 | 00 42 27.14  | 05 05 24.1  | 1.504 | 24.8     | 19.0 | 93                | 231               | 579              |
| 3   | 0126+0502 | 01 26 16.13  | 05 02 10.3  | 1.008 | 18.0     | 18.1 | 51                | 151               | 402              |
| 4   | 0143+0505 | 01 43 33.97  | 05 07 58.0  | 2.135 | 7.4      | 20.6 | 52                | 164               | 485              |
| 5   | 0226+0512 | 02 26 19.81  | 04 46 32.3  | 1.235 | 10.7     | 20.1 | 98                | 242               | 532              |
| 6   | 0459+0456 | 04 59 04.28  | 04 55 54.4  | 1.189 | 63.8     | 20.9 | 90                | 251               | 564              |
| 7   | 1100+0444 | 11 00 11.49  | 04 44 01.4  | 0.890 | 0.3      | 19.1 | 239               | 640               | 1453             |
| 8   | 1154+0431 | 11 54 53.50  | 04 24 12.5  | 0.998 | 6.7      | 19.9 | 331               | 854               | 1867             |
| 9   | 1251+0446 | 12 51 29.50  | 04 46 41.7  | 0.96  | 257      | 19.3 | 204               | 514               | 1611             |
| 10  | 1333+0451 | 13 33 07.00  | 04 50 48.6  | 1.405 | 129.5    | 17.3 | 21                | 55                | 123              |
| 11  | 1456+0456 | 14 56 25.79  | 04 56 44.8  | 2.13  | 2.2      | 20.0 | 110               | 288               | 727              |
| 12  | 1740+0502 | 17 40 33.96  | 05 02 42.3  | 3.57  | 4.7      | 22.6 | 36                | 110               | 288              |
| 13  | 2013+0508 | 20 13 23.48  | 05 10 30.5  | 0.89  | 10.0     | 21.1 | 53                | 138               | 281              |
| 14  | 2036+0451 | 20 36 56.93  | 04 49 52.7  | 0.716 | 56.0     | 19.0 | 80                | 228               | 563              |
| 15  | 2144+0513 | 21 44 27.18  | 05 11 15.2  | 1.01  | 1.9      | 18.8 | 66                | 203               | 526              |
| 16  | 2225+0523 | 22 25 14.72  | 05 27 09.1  | 2.323 | 2.7      | 17.8 | 309               | 849               | 2219             |
| 17  | 2320+0459 | 23 20 44.74  | 04 59 24.9  | 1.39  | 15.2     | 20.4 | 78                | 169               | 423              |

| No. | $\alpha_{3940}$ | $\alpha_{500}$ | $L_{3940}$<br>WHz <sup>-1</sup> | $L_{500}$<br>WHz <sup>-1</sup> | Morphology | Note             |
|-----|-----------------|----------------|---------------------------------|--------------------------------|------------|------------------|
| 1   | 11              | 12             | 13                              | 14                             | 15         | 16               |
| 1   | -1.08           | -0.776         | $2.68 \times 10^{27}$           | $1.25 \times 10^{28}$          | FR II D.   | B(Ly $\alpha$ )  |
| 2   | -0.937          | -0.836         | $7.61 \times 10^{26}$           | $4.32 \times 10^{27}$          | D, FR II   | B                |
| 3   | -1.133          | -0.874         | $1.99 \times 10^{26}$           | $1.31 \times 10^{27}$          | D, FR II   | B                |
| 4   | -1.245          | -0.926         | $1.31 \times 10^{27}$           | $8.47 \times 10^{27}$          | D, FR II   | B(Ly $\alpha$ )  |
| 5   | -0.947          | -0.686         | $5.33 \times 10^{26}$           | $2.34 \times 10^{27}$          | D, FR II   | B                |
| 6   | -1.167          | -0.615         | $5.27 \times 10^{26}$           | $2.14 \times 10^{27}$          | D, FR II   | B                |
| 7   | -0.874          | -0.874         | $5.98 \times 10^{26}$           | $3.63 \times 10^{27}$          | P          | B                |
| 8   | -0.994          | -0.682         | $1.15 \times 10^{27}$           | $5.22 \times 10^{27}$          | D, FR II   | B                |
| 9   | -1.129          | -0.875         | $7.12 \times 10^{26}$           | $4.74 \times 10^{27}$          | D, FR II   | B                |
| 10  | -1.09           | -0.702         | $1.69 \times 10^{26}$           | $7.07 \times 10^{26}$          | T,C,FR II  | B                |
| 11  | -0.875          | -0.875         | $1.80 \times 10^{27}$           | $1.19 \times 10^{28}$          | D?         | B                |
| 12  | -1.148          | -0.870         | $2.71 \times 10^{27}$           | $1.43 \times 10^{28}$          | CL         | B (Ly $\alpha$ ) |
| 13  | -0.809          | -0.809         | $1.27 \times 10^{26}$           | $6.74 \times 10^{26}$          | D, FR II   | B                |
| 14  | -1.076          | -0.816         | $1.40 \times 10^{26}$           | $8.58 \times 10^{26}$          | T,C,FR II  | B                |
| 15  | -1.066          | -1.066         | $2.47 \times 10^{26}$           | $1.97 \times 10^{27}$          | T,C,FR II  | B                |
| 16  | -0.995          | -0.902         | $7.04 \times 10^{27}$           | $4.50 \times 10^{28}$          | T,C,FR II  | B                |
| 17  | -0.868          | -0.769         | $5.05 \times 10^{26}$           | $2.52 \times 10^{27}$          | D, FR II   | B                |

Table 4. Radio galaxies with no emission lines detected.

| No. | RCJ name   | RA          | Dec        | $m_R$  | LAS   | $S_{3940}$<br>mJy |
|-----|------------|-------------|------------|--------|-------|-------------------|
| 1   | 2          | 3           | 4          | 5      | 6     | 7                 |
| 1   | 0015+0503a | 00 15 11.61 | 05 06 39.8 | 22.0   | 20.6  | 19                |
| 2   | 0250+0512  | 02 50 53.57 | 05 16 12.7 | >24.5  | 1.2   | 68                |
| 3   | 0308+0454  | 03 08 33.95 | 04 54 10.3 | 23.3   | 1.2   | 29                |
| 4   | 0324+0442  | 03 24 07.32 | 04 42 01.8 | 22.4   | 11.8  | 120               |
| 5   | 0355+0449  | 03 55 12.72 | 04 40 41   | 24.2   | 2.4   | 62                |
| 6   | 0446+0525  | 04 46 23.17 | 05 40 50.2 | 23.2   | 19.17 | 107               |
| 7   | 0743+0455  | 07 43 15.59 | 04 55 52.5 | 23.6   | 20.5  | 37                |
| 8   | 0836+0511  | 08 36 48.09 | 05 13 09.0 | 22.6   | 19.6  | 113               |
| 9   | 0945+0454  | 09 45 26.81 | 04 54 13.7 | 23.5   | 4.5   | 20                |
| 10  | 1051+0449  | 10 51 25.78 | 04 49 43.9 | 22.5   | 1.7   | 122               |
| 11  | 1148+0455  | 11 48 47.88 | 04 55 24.4 | 23.2   | 43.9  | 250               |
| 12  | 1152+0449  | 11 52 23.67 | 04 48 14.3 | 22.5   | 7.0   | 46                |
| 13  | 1703+0502  | 17 03 29.32 | 05 02 11.6 | 23.5   | 1.8   | 210               |
| 14  | 1720+0455  | 17 20 04.6  | 04 53 48.8 | (20.6) | 0.5   | 19                |
| 15  | 1735+0454  | 17 35 41.76 | 04 55 15.3 | 23.2   | 5.2   | 28                |
| 16  | 2219+0458  | 22 19 06.13 | 04 58 45.7 | 23.8   | 4.7   | 50                |
| 17  | 2236+0454  | 22 36 51.17 | 04 55 09.2 | 23.6   | 40.2  | 41                |

| No. | $\alpha_{3940}$ | $\alpha_{500}$ | Morphology         | Exposure time and note      |
|-----|-----------------|----------------|--------------------|-----------------------------|
| 1   | 8               | 9              | 10                 | 11                          |
| 1   | -1.67           | -1.03          | D, FR II           | 2×900s                      |
| 2   | -1.26           | -1.26          | D, FR II           | 4×900s                      |
| 3   | -0.965          | -0.965         | CL or D, BC, FR II | 4×900s, 3×1200s, 6×900s     |
| 4   | -1.131          | -0.974         | D, FR II/I         | 6×900s, 4×900s              |
| 5   | -1.494          | -1.296         | D, FR II           | 2×900s, 4×900s              |
| 6   | -0.983          | -0.983         | D, FR II           | 3×900s                      |
| 7   | -1.064          | -1.064         | D, FR II           | 2×900s                      |
| 8   | -1.05           | -1.05          | D, CJ, FR II/I     | 4×120s                      |
| 9   | -1.01           | -1.01          | D, FR II           | 4×900s                      |
| 10  | -0.92           | -0.92          | D, FR II           | 2×900s                      |
| 11  | -1.24           | -0.94          | D, FR II           | 2×900s                      |
| 12  | -0.762          | -0.762         | D, FR II           | 3×900s                      |
| 13  | -1.05           | -1.05          | D, FR II           | 3×900s, 2×600, 900s, 2×900s |
| 14  | -1.01           | -1.41          | P                  | 600s; M star by spectrum    |
| 15  | -0.924          | -0.924         | D, FR II           | 4×900s                      |
| 16  | -1.227          | -0.861         | D, FR II           | 2×900s                      |
| 17  | -1.517          | -0.899         | D, FR II           | 2×900s, 4×1200s             |

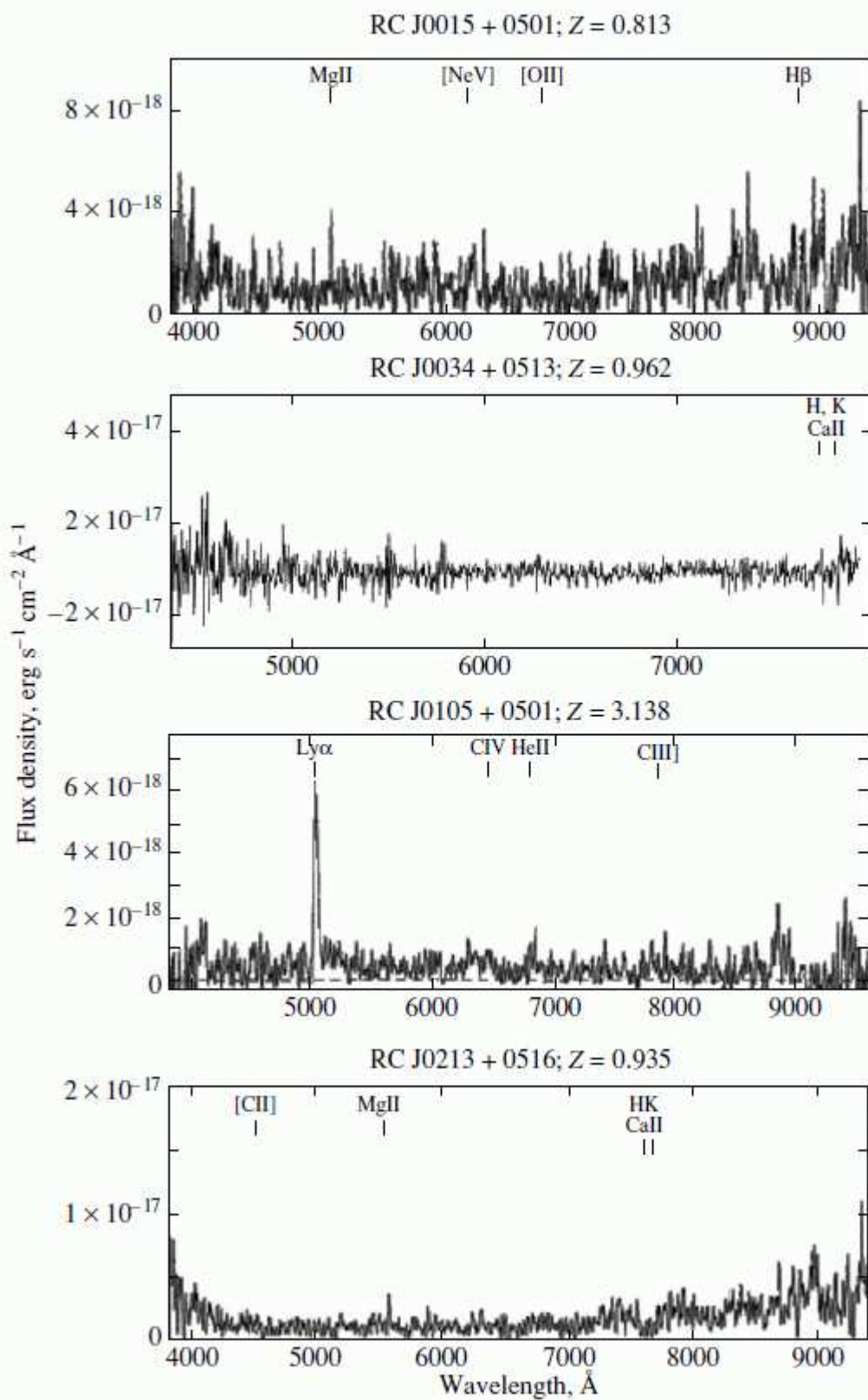


Figure 1: Spectra of radio galaxies with  $z > 0.7$ .

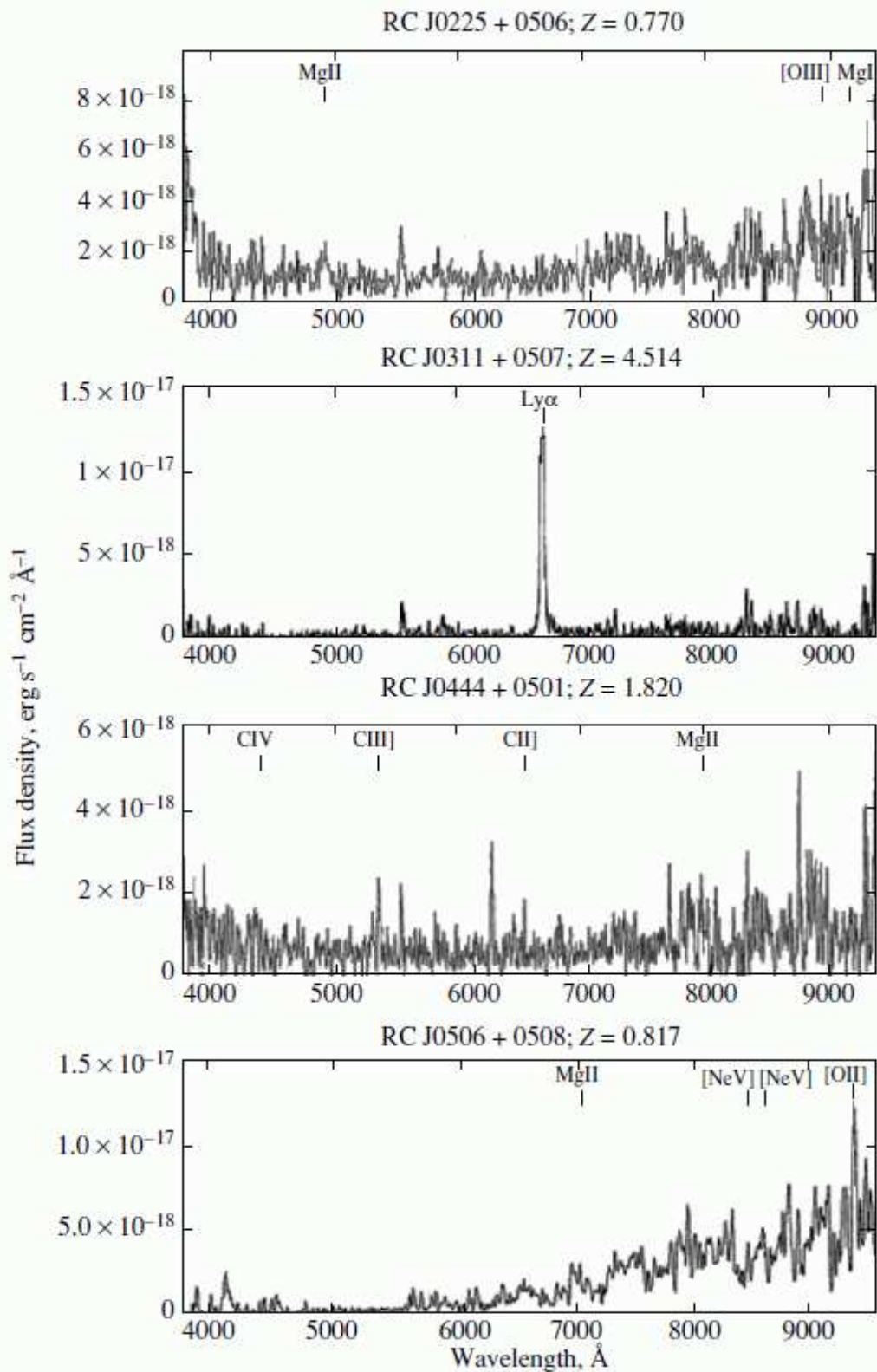


Fig. 1. (Continued)



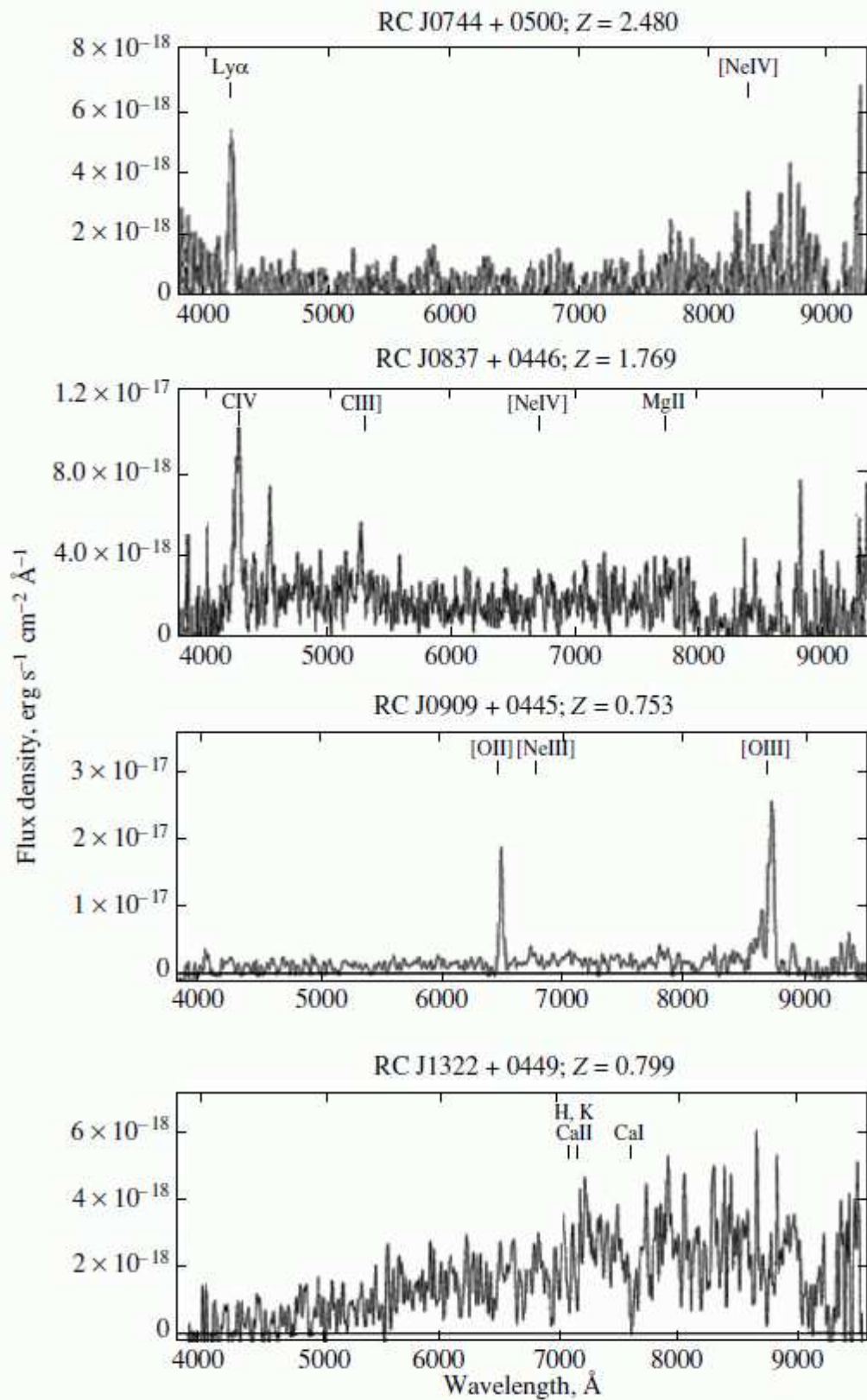


Fig. 1. (Continued)

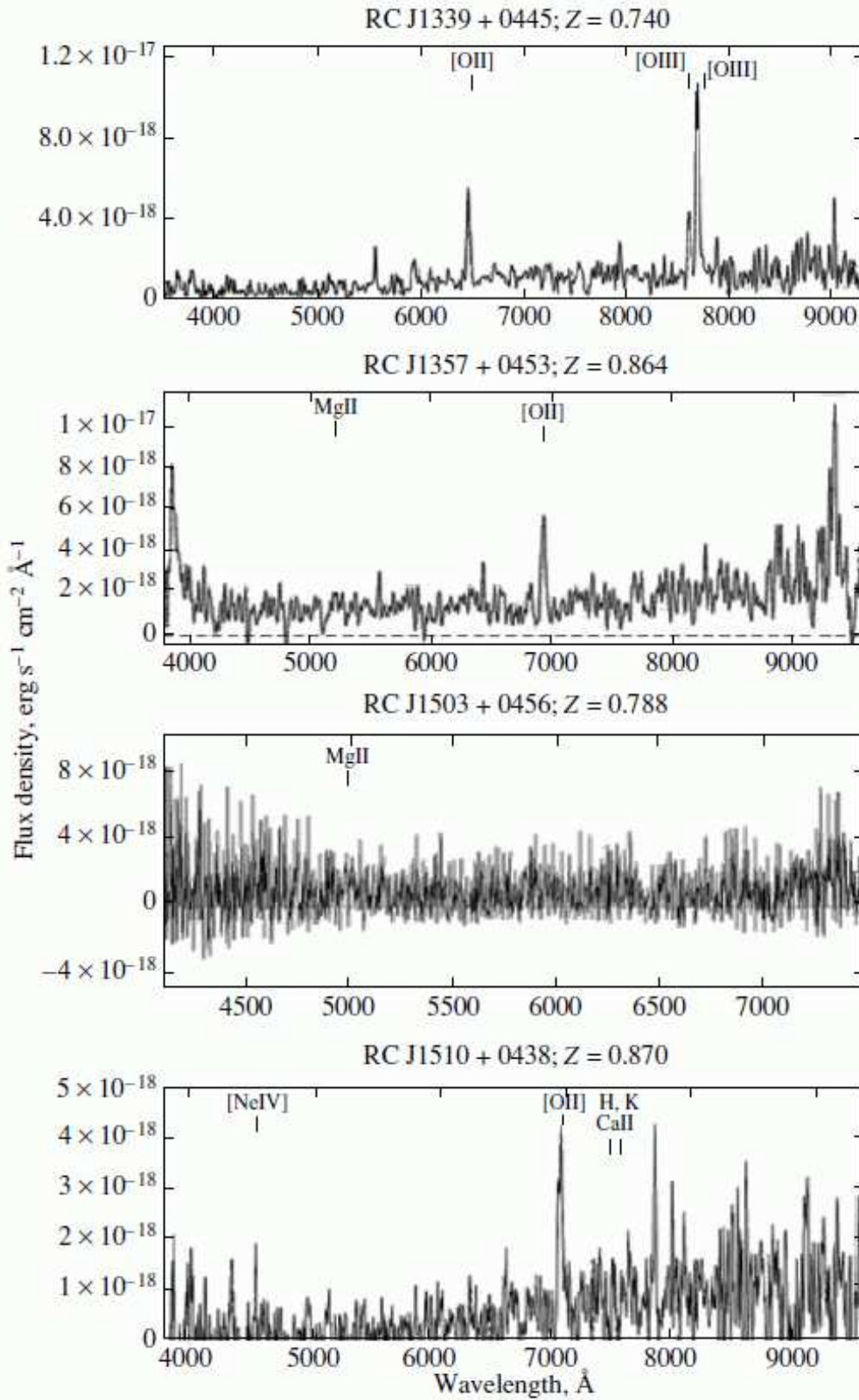


Fig. 1. (Continued)

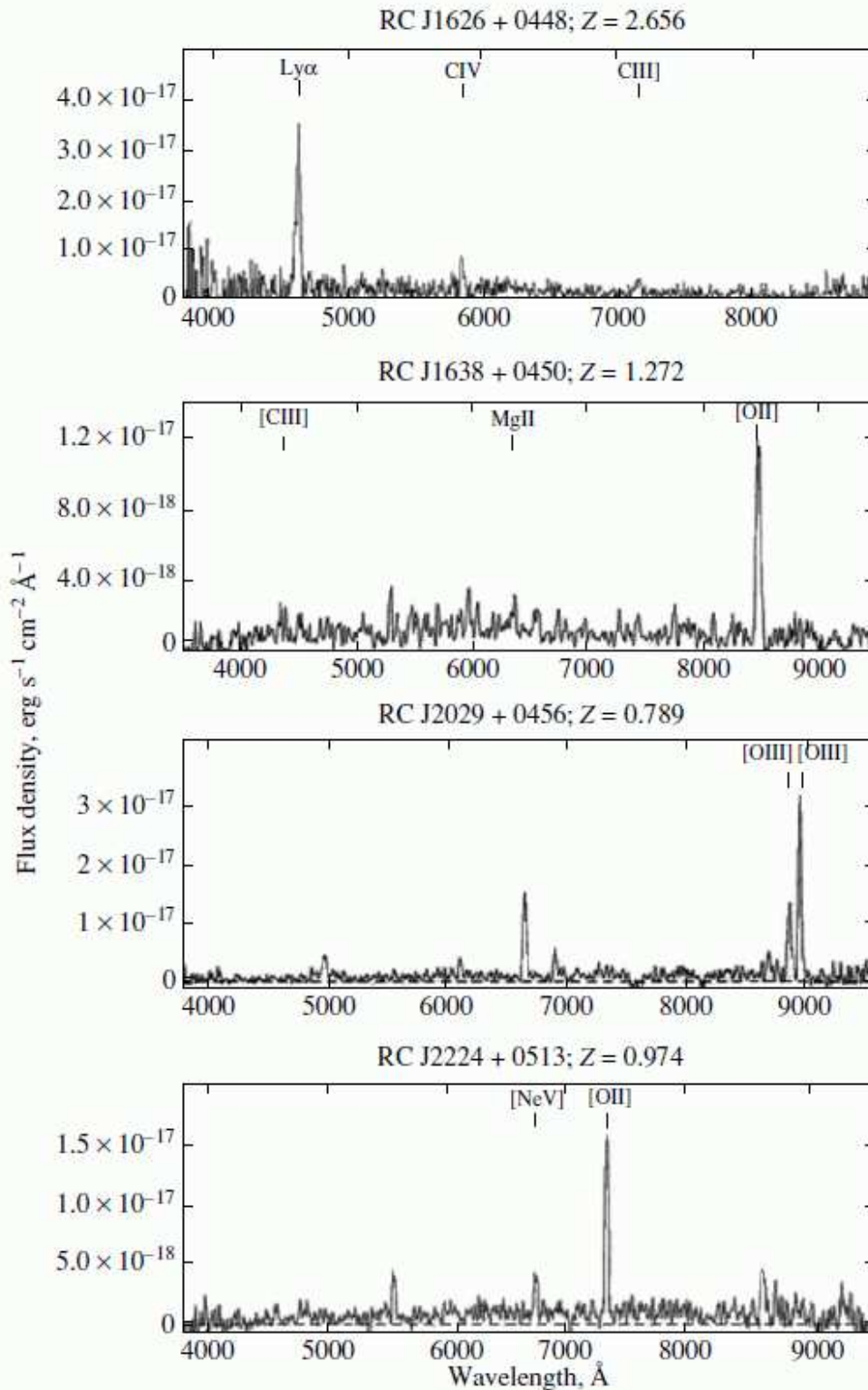


Fig. 1. (Continued)

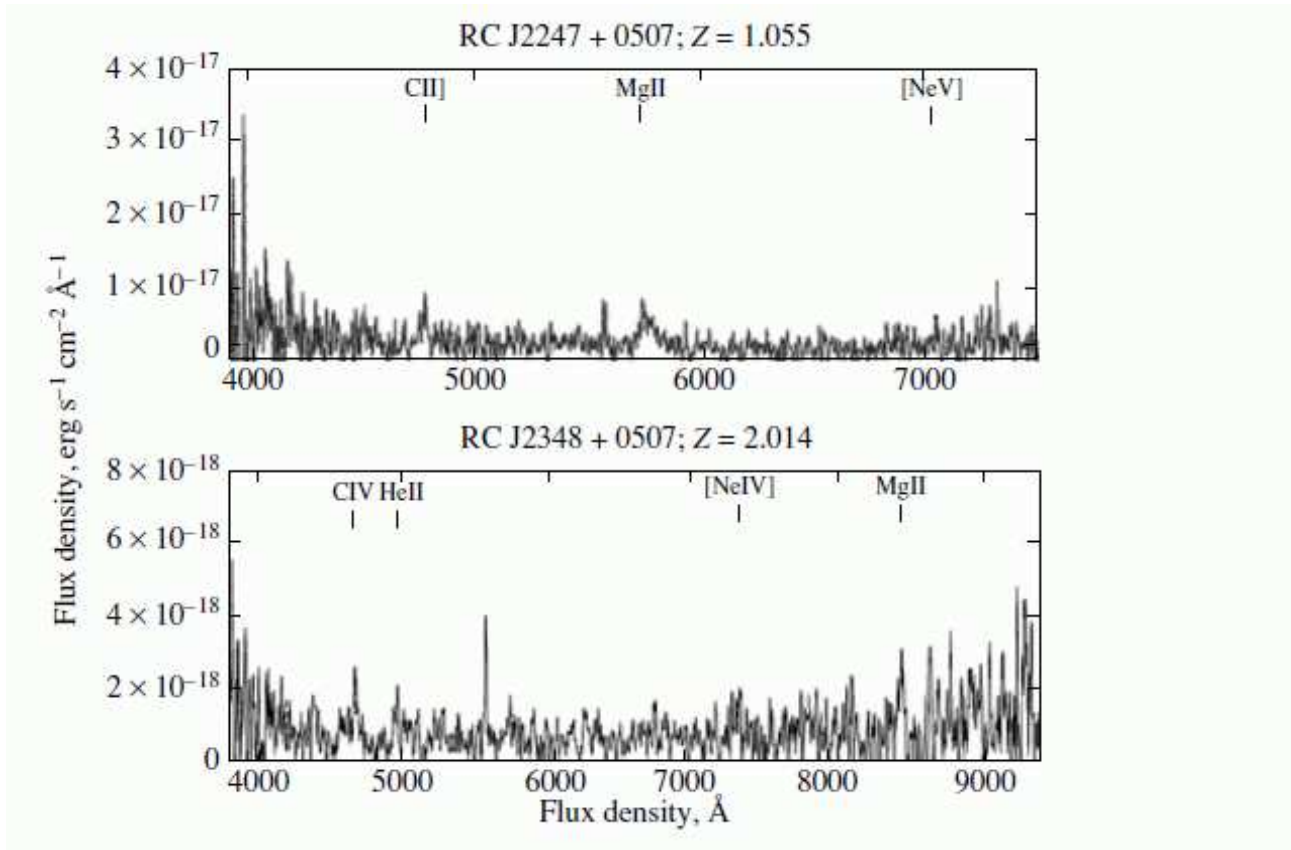


Fig. 1. (Continued)

source, ‘T’ a triple source, ‘C’ the presence of a core, ‘BC’ the presence of a bright core, ‘WC’ the presence of a weak core, ‘CL’ a core and lobe structure (distinct components), ‘CJ’ a core and jet structure (the core not distinguishable from the extended jet), and FRI/FRII an object of Fanaroff–Riley types I/II; 16 — notes, with n, B and abs indicating the presence of narrow emission lines, broad emission lines, and absorption lines in the spectrum and BLRG indicating a broad-line radio galaxy.

The columns of Table 3 contain the same information as in Tables 1 and 2 for the 17 detected quasars. Table 4 presents the results for the 17 radio galaxies without detected emission lines.

Columns 1–5 of Table 4 are analogous to the corresponding columns in Tables 1–3. The following columns contain: 6 — the largest angular size in arcseconds, LAS; 7 — the flux density,  $S$ , in mJy at 3940 MHz; 8, 9 — the spectral indices  $\alpha$  at 3940 and 500 MHz; 10 — the morphology; 11 — the exposure time, in seconds, and notes. Note that the absence of detectable lines for faint objects could, in some cases, be due to a higher redshift ( $z \geq 5$ ) or absorption by dust, or bad weather conditions (with seeing  $\sim 2''$ – $3''$ ). One can not also exclude an incorrectly placed spectrograph slit. For example, such objects in Table 4 include RCJ 0250+512 and RCJ 0355+0449, whose spectral indices, morphologies, angular sizes, and ratios of the radio to optical luminosity suggest they may be very distant objects. It would be desirable to obtain spectroscopy of these objects using telescopes with higher sensitivities and broader frequency ranges, repeat the 6-m SAO observations under very good seeing conditions, or obtain observations in the K-filter.

Below we present remarks for several of the radio sources.

**RCJ 0015+0503a** (Table 4). This object has  $B=23.98$ ,  $V=23.04$ ,  $R=22.26$ ,  $I=21.40$ . The observing conditions were poor, with seeing of  $\sim 3''$ ;  $z_{ph}=0.60\pm 0.13$ .

**RCJ 0034+0513** (Table 1). The redshift was measured from two absorption lines, at  $7700\text{ \AA}$  (the KCaII 3933.7  $\text{\AA}$  line) and  $7800\text{ \AA}$  (the HCaII 3968.5  $\text{\AA}$  line);  $z_{ph}=1.03$ .

**RCJ 0105+0501** (Table 1). The radio source is double; it is not clear where the AGN is located. An optical object displaying Ly $\alpha$  emission has the coordinates  $\alpha=01h05m34.091s$ ,  $\delta=+5^\circ 01' 12.47''$  (J2000), not coincident with any of the radio components. Radio observations with higher sensitivity and resolution are desirable, in order to detect the radio core. The object's has  $B=24.1$ ,  $V=22.5$ ,  $R=22.8$ ,  $I=22.4$ .

**RCJ 0213+0516** (Table 1). The object is a cluster member. The brightest member of the cluster is a radio quasar at redshift  $z_{sp} = 0.94$  (approximately the same  $z$  as for the FRII radio galaxy),  $8''$  to the east of the radio core. The contribution from the compact core is about 3% of the total flux density of the radio source. There is a small jet directed away from the quasar. Interaction between the quasar and the host galaxy cannot be ruled out. (The VLA radio image with overlaid 6-m SAO optical image can be found at <http://wo.sao.ru/hd/zhe>; similar information is also available for other objects at this same address.)

**RCJ 0311+0507** (Table 1). This object has the highest redshift in our sample [26, 27]. It has  $B>24.9$ ,  $V>24.8$ ,  $R=22.6$ ,  $I=22.3$ . This radio source has now been studied using the “Merlin” radio interferometer (UK) and European VLBI Network (EVN).

**RCJ 0324+0442** (Table 4). This is an FRII double radio source, most probably in an empty field (the two galaxies near the eastern component are foreground objects);  $m_R>25$ . If such objects are detected in the K-band at the level  $K=18\text{--}19$ , they enter the range  $z_{sp}=1.5\text{--}2$ , and have no bright emission lines in the optical.

**RCJ 0506+0508** (Table 1). The redshift was determined from absorption lines at  $7150\text{--}7250\text{ \AA}$  (though there remain some doubts).

**RCJ 0836+0511** (Table 4). This is not an entirely classical FRII object: the radio map at  $8460\text{ MHz}$  (VLA) reveals a core, a jet toward the Northeast, a hot spot, and a “tail”;  $z_{ph}=1.12$ .

**RCJ 0908+0451** (Table 2).  $z_{sp}=0.542$ , based on data from the NASA Extragalactic Database (NED).

**RCJ 1011+0502** (Table 2). This is the faintest galaxy among the RC objects, with the lowest luminosity in the optical (possibly a Sy1 galaxy with a strong jet).

**RCJ 1051+0449** (Table 4). The direct images give  $B=23.77$ ,  $V=23.12$ ,  $R=22.74$ , while the object was not detected in the I-band (the images were taken in the presence of seeing of  $1.5''$ ); no images of a BVRI standard were taken, and the reduction was made using surrounding SDSS objects.

**RCJ 1100+0444** (Table 3). The NED-based redshift is  $z_{sp}=0.8861$ .

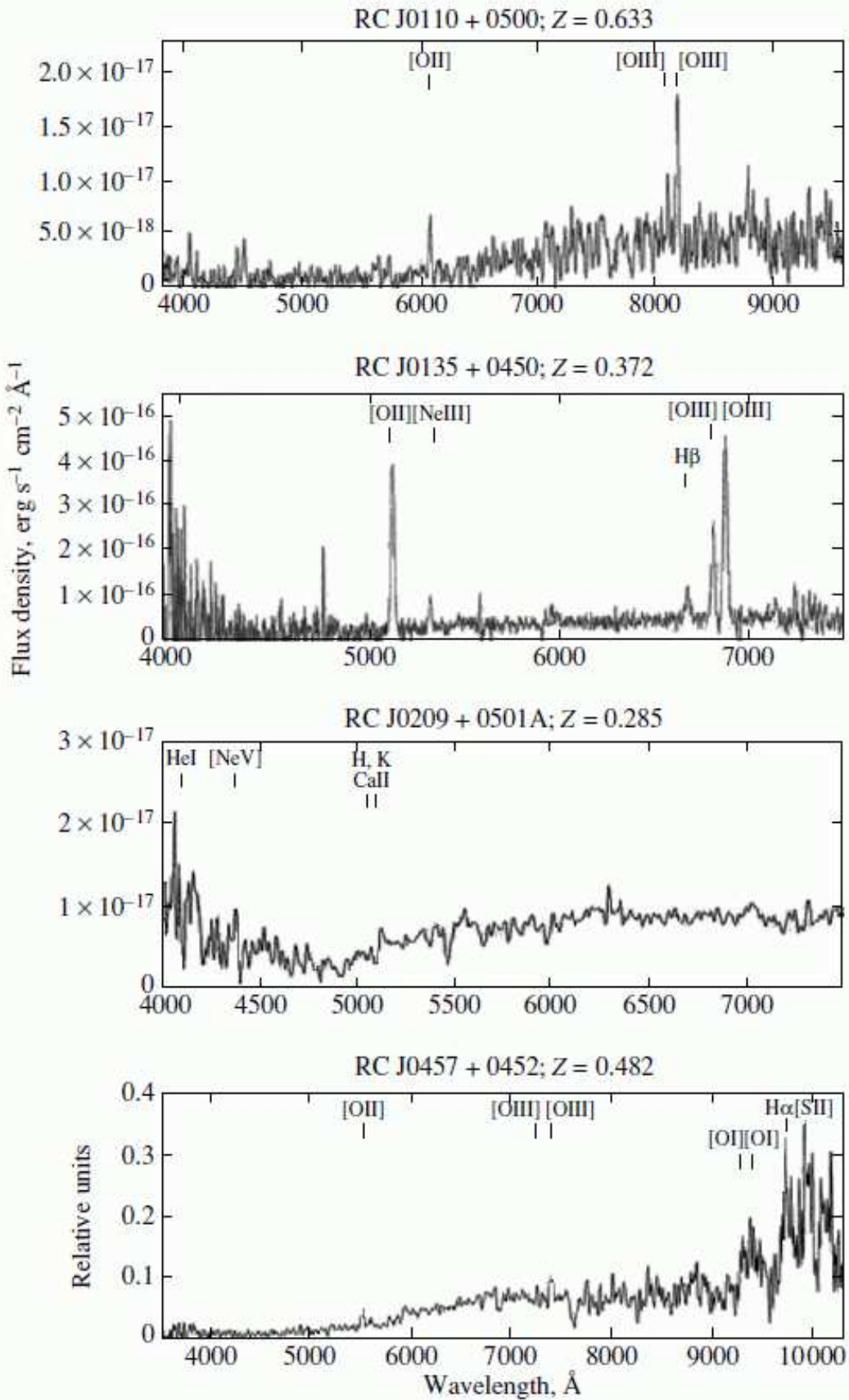
**RCJ 1124+0456** (Table 2). The NED-based redshift is  $z_{sp}=0.2827$ .

**RCJ 1148+0455** (Table 4). The NED redshift,  $z_{sp}=0.42$ , is not confirmed.

**RCJ 1152+0442** (Table 4). The photometric redshift  $z_{ph}=1.24$ , disagrees with our results.

**RCJ 1333+0451** (Table 3). The NED-based redshift is  $z_{sp}=1.4024$ ;  $z_{ph}=1.07$ .

**RCJ 1503+0456** (Table 1). It is more likely that the broad emission line at  $5002\text{ \AA}$  is MgII 2798  $\text{\AA}$  than CIII] 1909  $\text{\AA}$ . The MgII identification is favored, with a possibly detected continuum jump redward of  $7150\text{ \AA}$  ( $z_{sp}=0.788$ ). This is a BLRG, consistent with its magnitude and radio morphology (core+jet);  $z_{ph}=0.88$ .

Figure 2: Spectra of radio galaxies with  $z \geq 0.7$ .

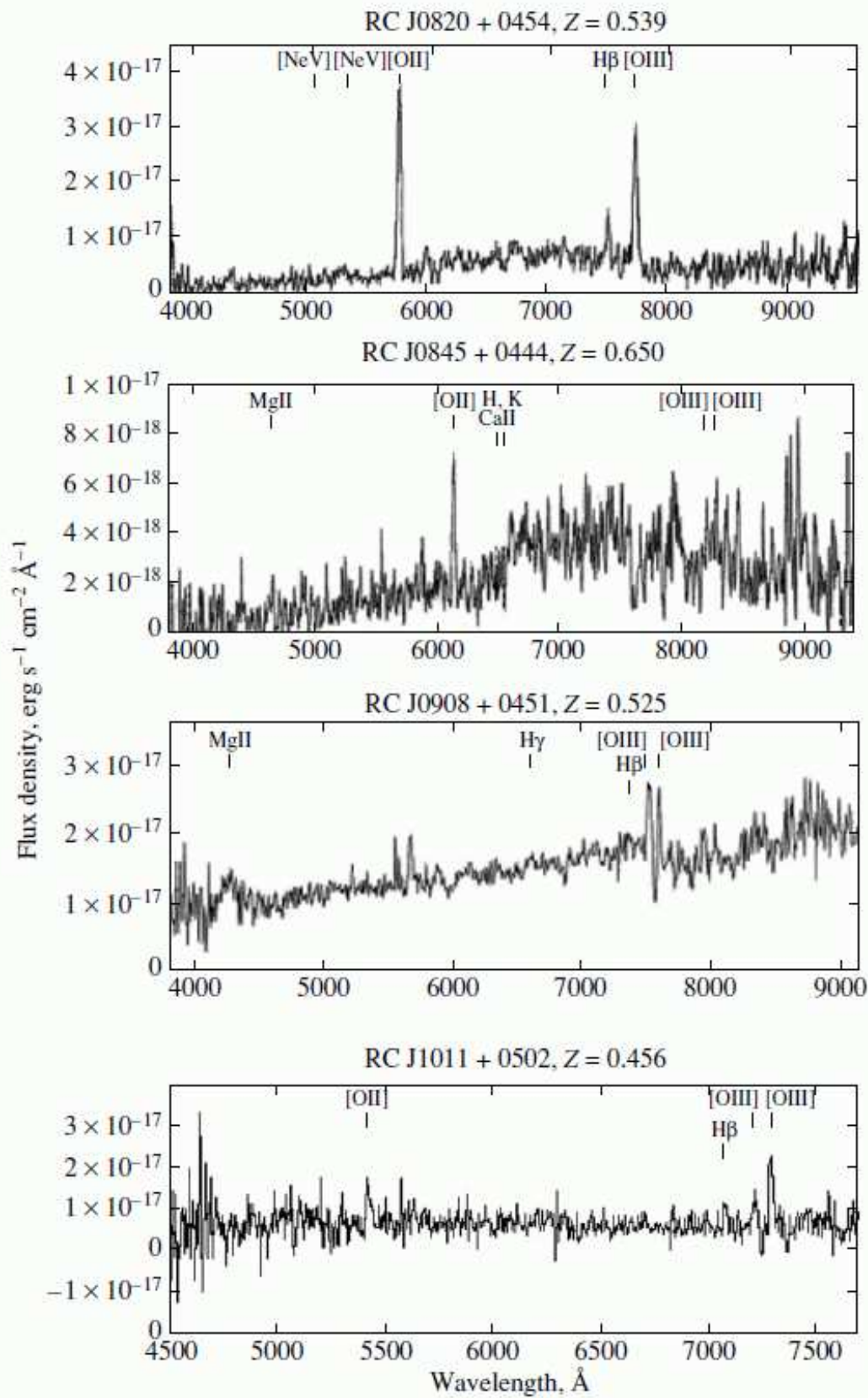


Fig. 2. (Continued)

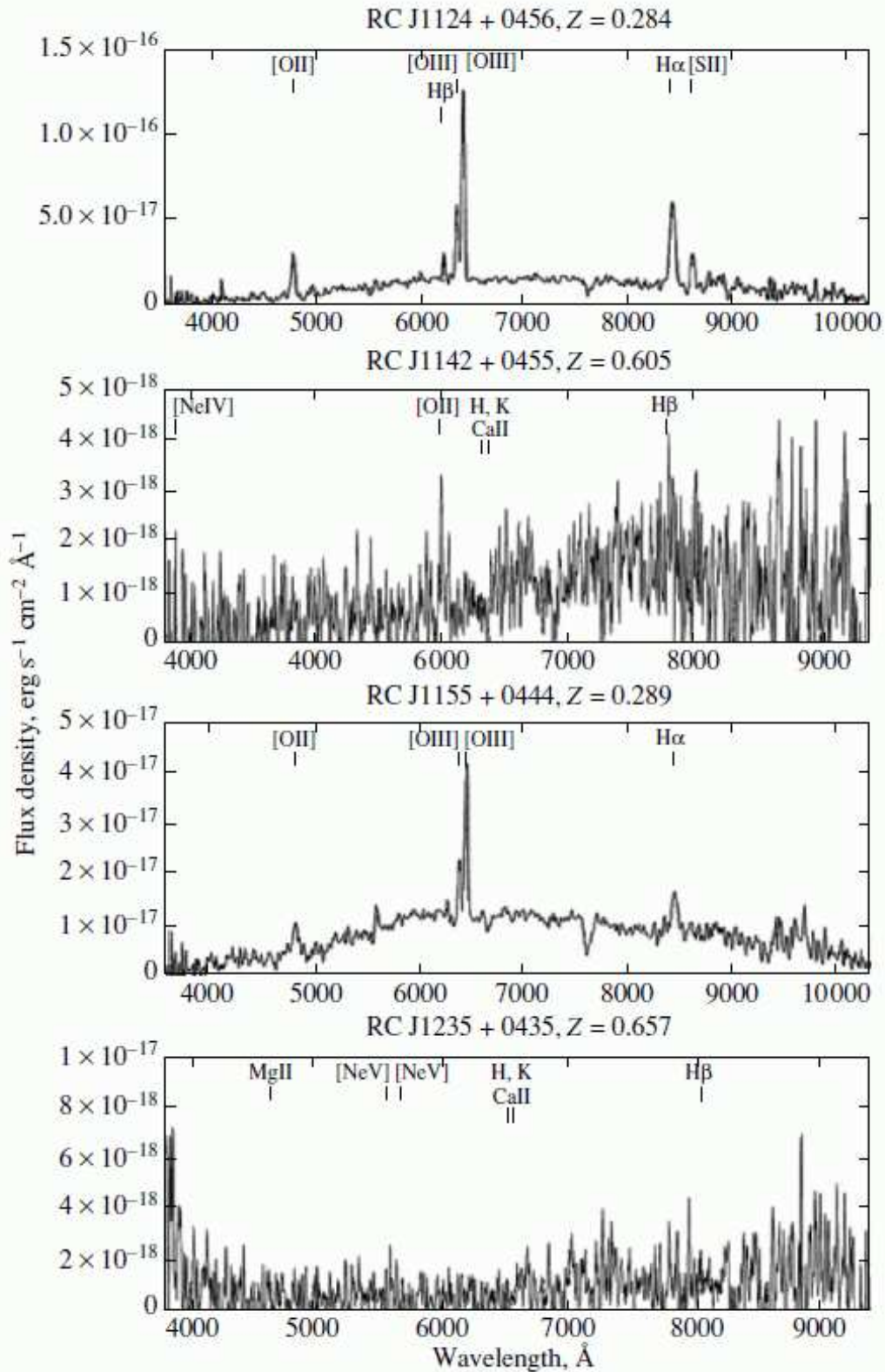


Fig. 2. (Continued)



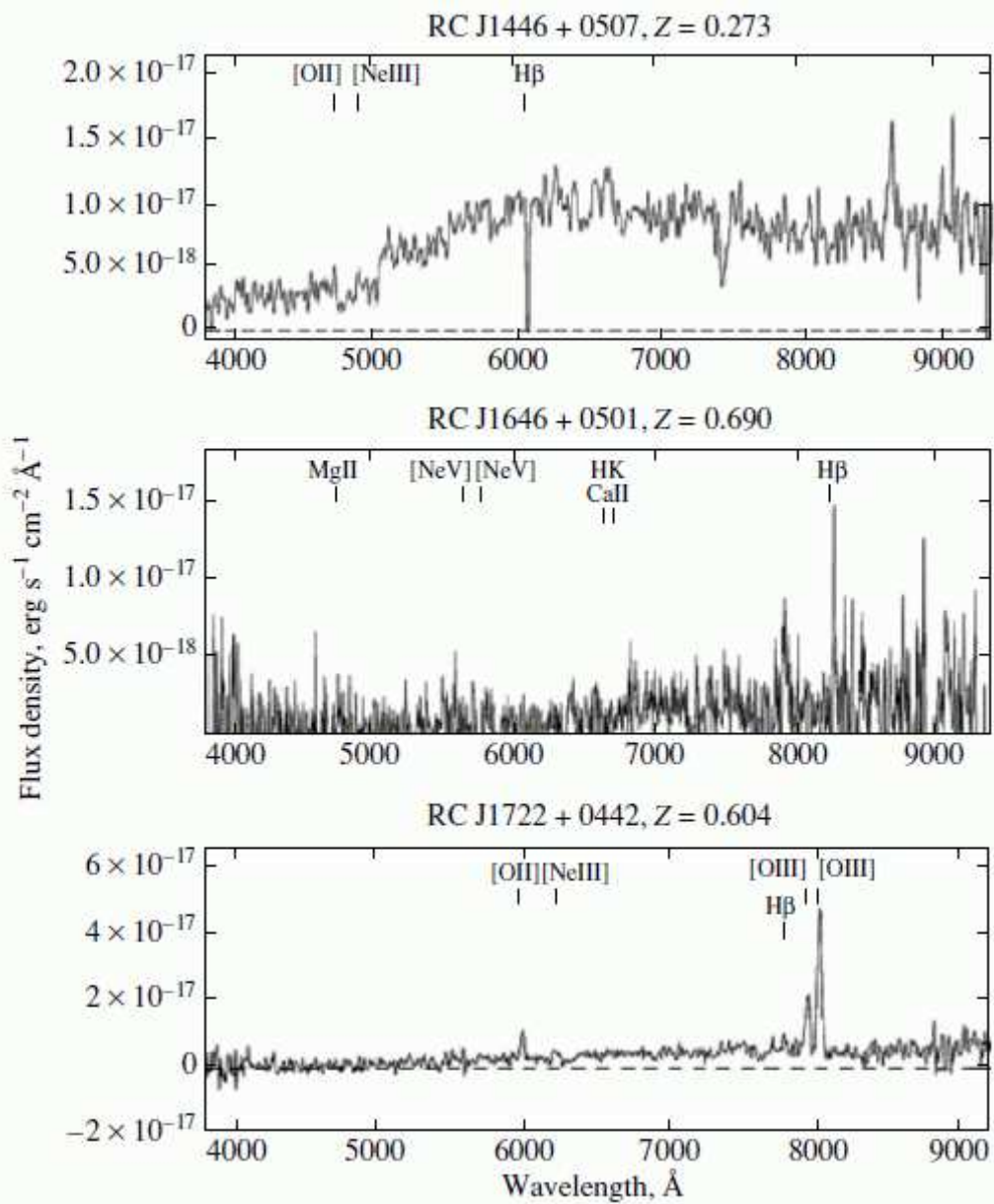


Fig. 2. (Continued)

**RCJ 1735+0454** (Table 4). No continuum or bright emission lines were detected. If the weak emission at 7274 Å is [OII] 3727 Å, then the redshift is  $z_{sp}=0.952$ . However, the spectrum to the red is too short to see the continuum jump and confirm this hypothesis.

**RCJ 1740+0502** (Table 3). This object has a broad Ly $\alpha$  line (5560 Å) but no CIV line. This is a star-like object in the optical, i.e., with a dominant nucleus. However, it is not a typical quasar; such objects are sometimes called WQs (weak quasars).

**RCJ 2219+0458** (Table 4). The continuum grows to the blue, in contradiction with the galaxy's colors (B=24.8, V=25.03, R=23.72, I=22.25);  $z_{ph} = 1.24$ .

**RCJ 2225+0523** (Table 3). The NED-based redshift is  $z_{sp} = 2.323$ .

**RCJ 2247+0507** (Table 1). The spectrum contains a single broad emission line, MgII 2798 Å.

The optical spectra of radio galaxies with  $z > 0.7$  and  $z < 0.7$  are shown in Figs. 1 and 2. Figure 3 displays the spectra of the quasars.

Thus, among the 22 radio galaxies in Table 1, we detected one object with  $z = 4.51$ , one with  $3 \leq z < 4$ , three with  $2 \leq z < 3$ , and four with  $1 \leq z < 2$ . Three more objects have redshifts close to unity ( $>0.9$ ). The redshifts of 10 sources are in the range from 0.74 to 0.87. The redshifts of the 15 radio galaxies from Table 2 are between 0.27 and 0.69. Note that there are no objects with  $LAS > 12$  among the nine radio galaxies with  $z > 1$ . The 500-MHz spectral indices of the objects with  $z > 1$  are the same as or lower than their spectral indices at 3940 MHz. As a rule, the spectral indices of such objects at 3940 MHz exceed unity. Two of the three objects with  $z > 3$  (RCJ 0105+0501 and RCJ 1740+0502) have CL (core and lobe) structure, while the third object (RCJ 0311+0507) is a strongly asymmetric triple, almost a CL source.

One object among the 17 quasars has  $z=3.57$  (RCJ 1740+0502), four have  $2 \leq z < 3$ , seven have  $1 \leq z < 2$ , four have  $0.89 \leq z < 1$ , and one has  $z=0.72$ .

Figures 4 and 5 display the redshift distributions of the radio galaxies and quasars.

### 3. CONCLUSIONS

The “Big Trio” project includes about 100 objects, for 71 of which we have obtained optical spectra with the “Scorpio” spectrograph mounted on the 6-m telescope of the SAO (17 quasars and 54 radio galaxies).

Of the studied radio galaxies, four have redshifts  $1 \leq z < 2$ , three have  $2 \leq z < 3$ , one has  $3 \leq z < 4$ , and one has  $z=4.51$ . Thirteen sources have  $0.7 < z < 1$  and 15 have  $0. < z < 0.7$ . Five of the program quasars have  $0.7 < z < 1$ , seven have  $1 \leq z < 2$ , four have  $2 < z < 3$ , and one has  $z = 3.57$ . We detected no spectral lines for 17 objects.

Among the studied steep and ultra-steep spectrum radio sources with measured redshifts  $z$  (54 objects), we found  $\sim 39\%$  to have  $z > 2$ ,  $\sim 6\%$  to have  $z > 3$ , and  $\sim 2\%$  to have  $z > 4.5$  (4.514). The total number of radio galaxies with redshifts  $z > 4$  detected to date is currently six [28].

The failure to detect spectral lines in the spectra of 17 radio galaxies may indicate that they have redshifts in the range of  $1.5 < z < 2$  or  $z > 5$ , or may be due to absorption by dust. In some cases, observational errors or poor weather conditions could also be responsible.

Our data confirm the effectiveness of identifying candidate distant objects based on the properties of their radio and optical continua (steep radio spectra, characteristics of FR II objects, small angular sizes, large ratios of the radio and optical luminosities). These criteria

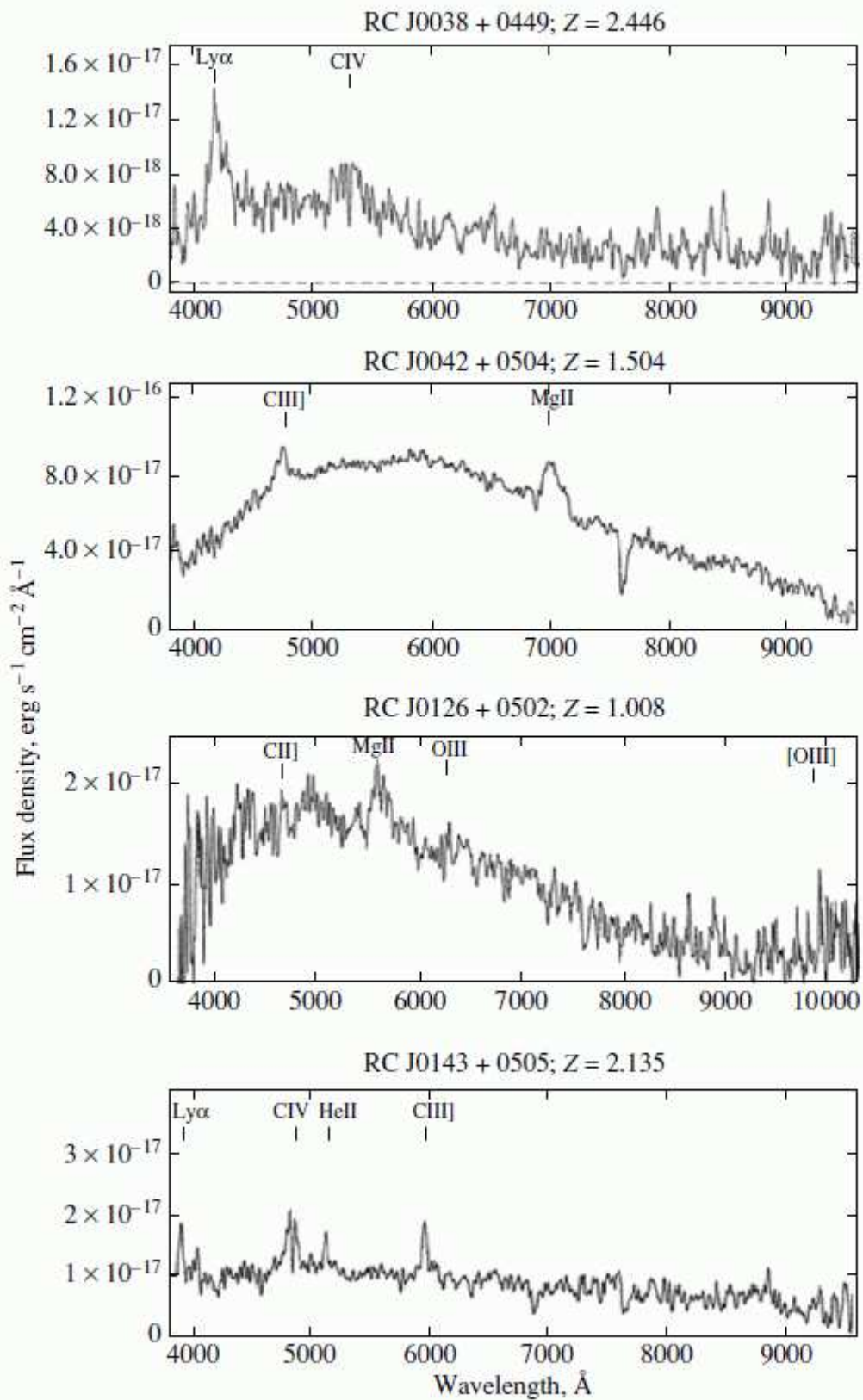
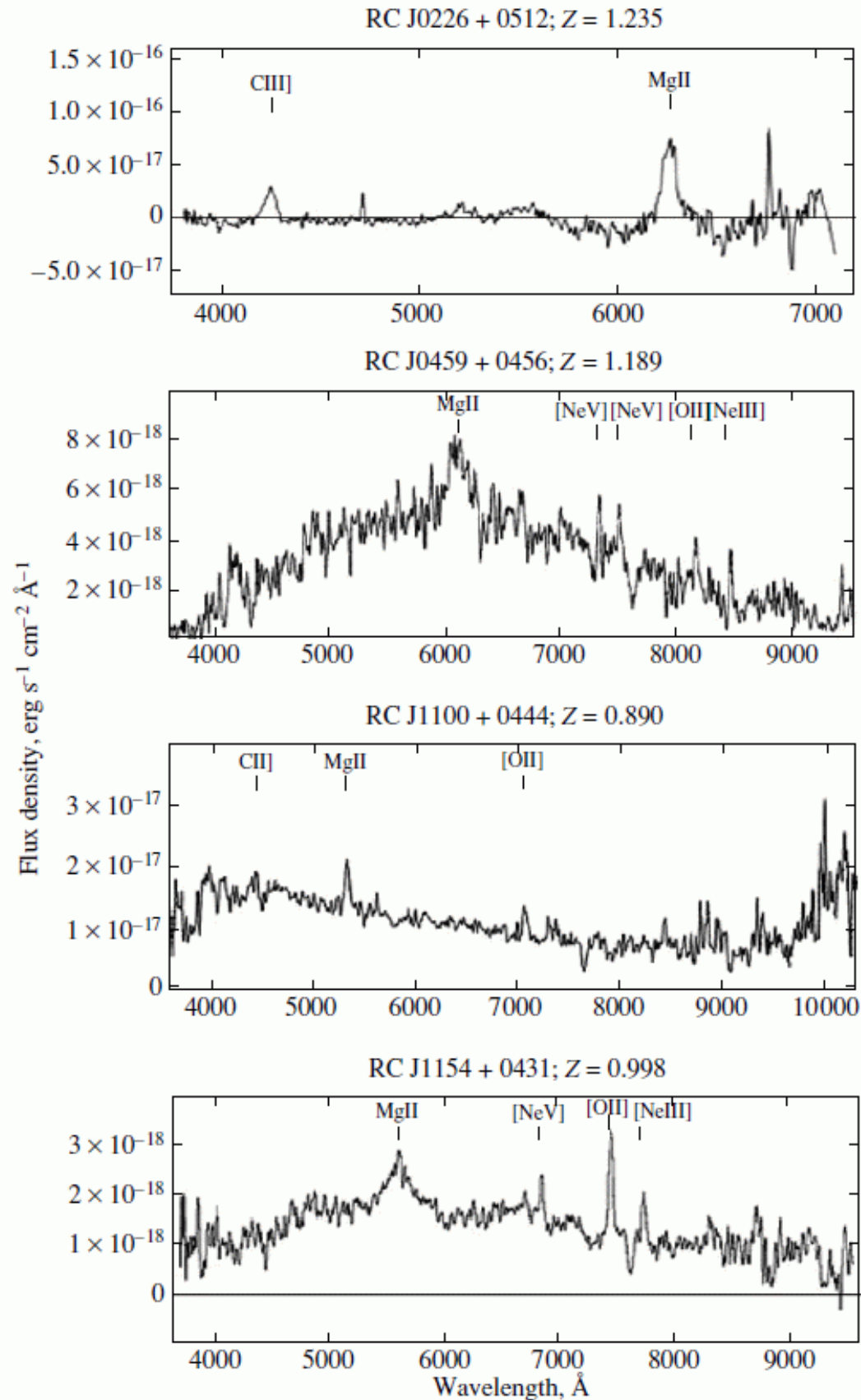


Figure 3: Spectra of quasars.

Fig. 3. (Continued)



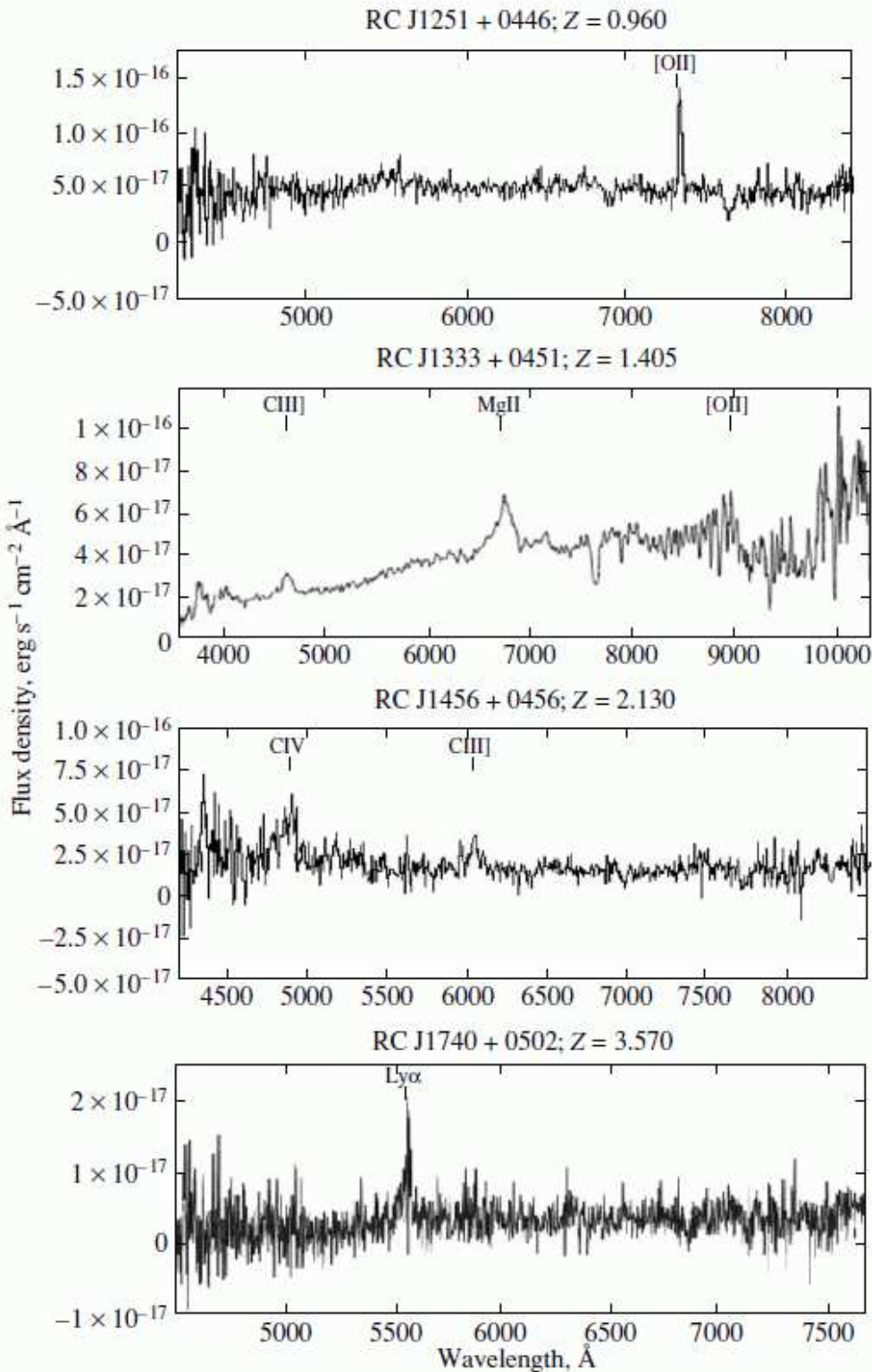


Fig. 3. (Continued)

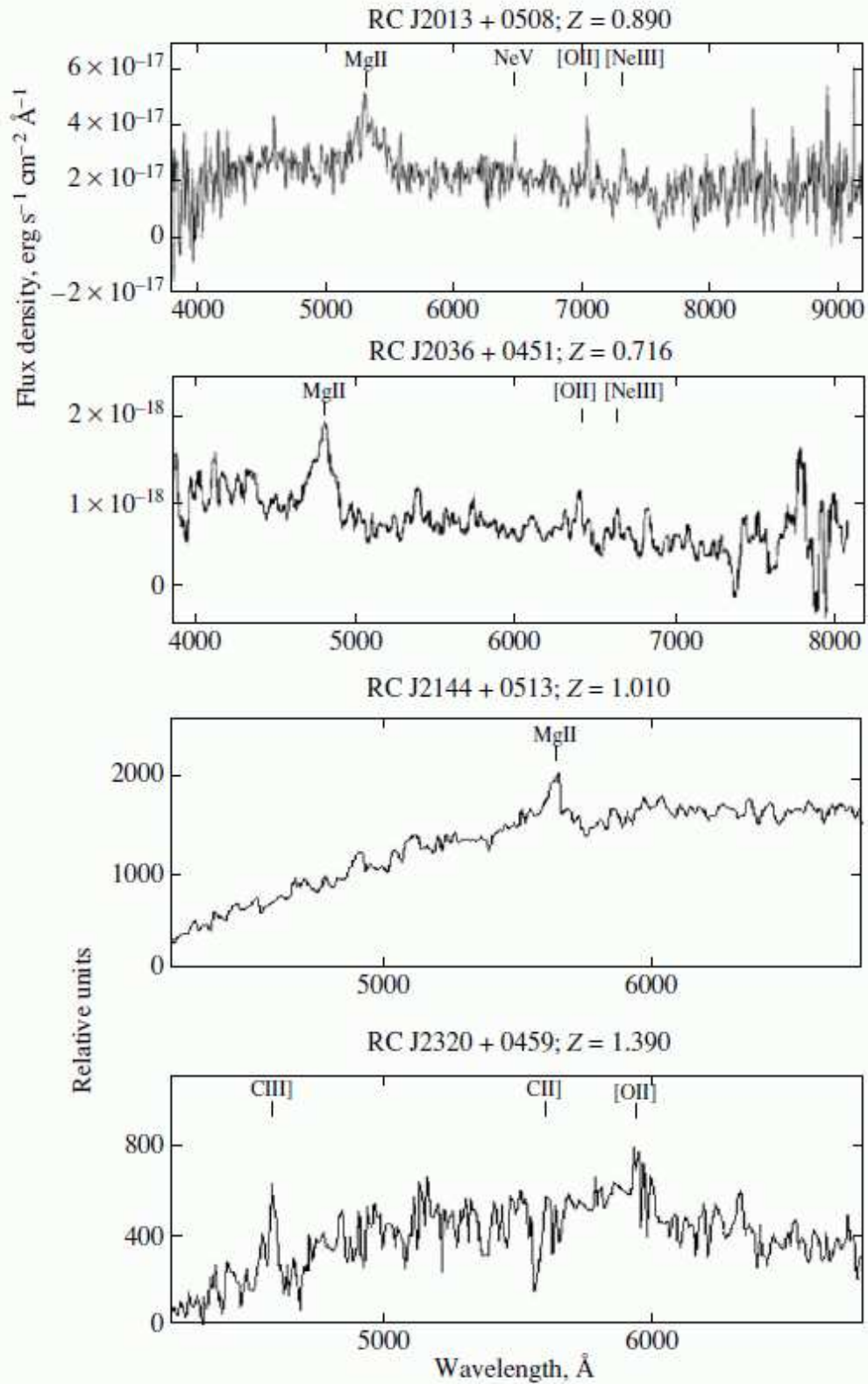


Fig. 3. (Continued)

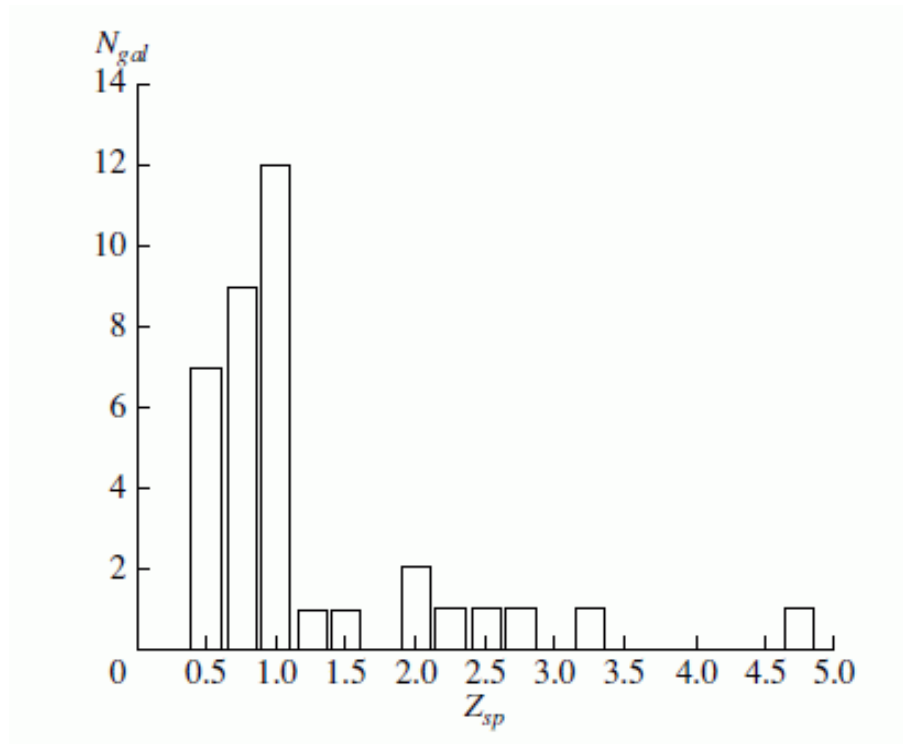


Figure 4: Redshift distribution of the galaxies.

made it possible to detect the object RCJ 0311+0507 with  $z = 4.514$ , which has a very high radio luminosity at centimeter wavelengths. Note that, since there are no selection effects, the fraction of distant objects in modern radio surveys (such as the NVSS) is much lower than the fraction in Fig. 4 resulting from the “Big Trio” program (see also the review by Pedani [29]). The identification of FR II radio sources at high redshifts is also helpful for searches for early “giant black holes” or first-generation clusters of galaxies.

We have presented here factual information on the 71 studied “Big Trio” objects. We are planning to discuss astrophysical implications of these data in future publications.

### Acknowledgments

This study was partially supported by the Russian Foundation for Basic Research (project nos. 08-02-00486a, 09-07-00320) and the Program of State Support of Leading Scientific Schools of the Russian Federation. The authors thank the observers at the 6-m telescope of the SAO who performed the observations with the “Scorpio” spectrograph. The Very Large Array of the National Radio Astronomy Observatory is a Facility of the National Science Foundation operated under cooperative agreement by Associated Universities, Inc., a science management corporation.

### References

- [1]. W. M. Goss, Y. N. Parijskij, A. I. Kopylov, et al., Turkish J. Phys. **18**, 894 (1994).
- [2]. O. V. Verkhodanov and Yu. N. Parijskij, Radio Galaxies and Cosmology (Fizmatlit, Moscow, 2009) [in Russian].
- [3]. Y. N. Parijskij and D. V. Korolkov, Astrophys. Space Phys. Rev. **5**, 40 (1986).
- [4]. Yu. N. Parijskij and D. V. Korolkov, Soobshch. Spets. Astrofiz. Observ. **12**, 5 (1984).

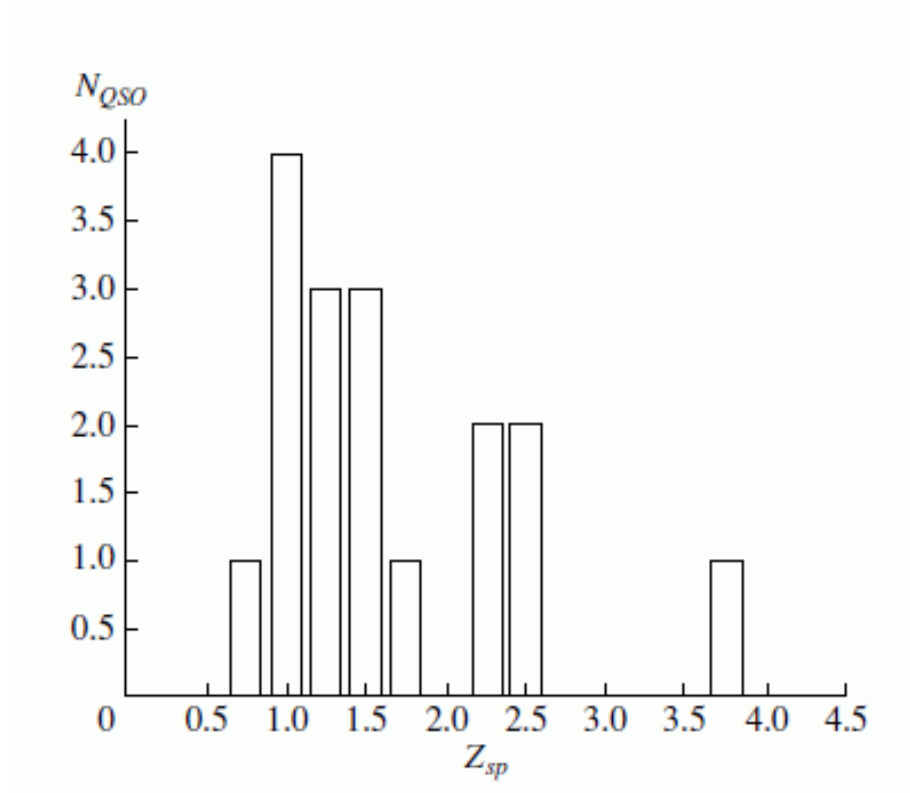


Figure 5: Redshift distribution of the quasars.

- [5]. Yu. N.Parijskij, N.N. Bursov, N. M. Lipovka, et al., *Astron. Astrophys. Suppl. Ser.* **87**, 1 (1991).
- [6]. Yu. N.Parijskij, N.N. Bursov, N. M. Lipovka, et al., *Astron. Astrophys. Suppl. Ser.* **96**, 583 (1992).
- [7]. V. K. Kapahi and V.K.Kulkarni, *Astron.J.* **99**, 1397 (1990).
- [8]. P. J. McCarthy, *Ann. Rev. Astron. Astrophys.* **31**, 639 (1993).
- [9]. A. I. Kopylov, W. M. Goss, Yu. N. Parijskij, et al., *Astron. Zh.* **72**, 613 (1995) [*Astron. Rep.* **39**, 543 (1995)].
- [10]. Yu.N.Parijskij, W.M. Goss, A. I. Kopylov, et al., *Astron. Zh.* **75**, 483 (1998) [*Astron. Rep.* **42**, 425 (1998)].
- [11]. T. Pursimo, K. Nilson, P. Teerikorpi, et al., *Astron. Astrophys. Suppl. Ser.* **134**, 505 (1999).
- [12]. O. V. Verkhodanov, A. I. Kopylov, Yu. N. Parijskij, et al., *Astron. Zh.* **79**, 589 (2002) [*Astron. Rep.* **46**, 531 (2002)].
- [13]. O. V. Verkhodanov, Yu.N.Parijskij, N.S.Soboleva, et al., *Bull. Spec. Astrophys. Observ.* **52**, 5 (2001).
- [14]. S. N. Dodonov, Yu.N.Parijskij, W. M.Goss, et al., *Astron. Zh.* **76**, 323 (1999) [*Astron. Rep.* **43**, 275 (1999)].
- [15]. V. L. Afanasiev, S. N. Dodonov, A. V. Moiseev, et al., *Astron. Zh.* **80**, 409 (2003) [*Astron. Rep.* **47**, 377 (2003)].
- [16]. W. M. Goss, Yu. N. Parijskij, N. S. Soboleva, et al., *Astron. Zh.* **69**, 673 (1992) [*Sov. Astron.* **36**, 343 (1992)].
- [17]. Yu. N. Parijskij, W. M. Goss, A. I. Kopylov, et al., *Bull. Spec.Astrophys.Observ.* **40**, 5 (1996).
- [18]. Yu. N. Parijskij, W. M. Goss, A. I. Kopylov, et al., *Bull. Spec.Astrophys.Observ.* **40**, 1 (1996).
- [19]. Yu.N.Parijskij, W.M. Goss, A. I. Kopylov, et al., *Astron. Astrophys. Trans.* **18**, 437 (1999).
- [20]. Yu. N. Parijskij, N. S. Soboleva, A. I. Kopylov et al., *Pisma Astron. Zh.* **26**, 493 (2000) [*Astron.*



- Lett. **26**, 423 (2000)].
- [21]. N. S. Soboleva, W. M. Goss, O. V. Verkhodanov, et al., Pisma Astron. Zh. **26**, 723 (2000) [Astron. Lett. **26**, 623 (2000)].
- [22]. Yu.N.Parijskij, W.M.Goss, A. I. Kopylov, et al., Astron. Astrophys. Trans. **19**, 297 (2000).
- [23]. Yu.N.Parijskij, N.S. Soboleva, W. M. Goss, et al., in Extragalactic Radio Sources, Ed. by R. Ekers et al. (Dordrecht, 1995), p. 591.
- [24]. T. Pursimo, K. Nilson, P. Teerikorpi, et al., in Proc. of the 8th Russ.–Finn. Symp. on Astronomy (St. Petersburg, 1999), p. 95.
- [25]. A. I. Kopylov, V. M. Goss, and Yu. N. Parijskij, Pisma Astron. Zh. **32**, 483 (2006) [Astron. Lett. **32**, 433 (2006)].
- [26]. Yu.N.Parijskij, N.S.Soboleva, A. V. Temirova, and A. I. Kopylov, Astron. Zh. **71**, 821 (1994) [Astron. Rep. **38**, 731 (1994)].
- [27]. A. I. Kopylov, Yu.N.Parijskij, N.S.Soboleva, et al., in Galaxy Evolution across the Hubble Time, Ed. by F. Combes and J. Palous (Cambridge Univ., Cambridge, 2007), p. 431.
- [28]. G. Miley and C. de Breuck, Astron. Astrophys. Rev. **15**, 67 (2008).
- [29]. M. Pedani, New Astron. **8**, 805 (2003).

*Translated by N. Samus.*